Guided Waves Benchmark Dataset

Ziemowit Dworakowski, Jakub Gorski, and Mateusz Heesch

AGH University of Science and Technology

Michal Dziendzikowski

Air Force Institute of Technology

June 24, 2022

Abstract

This report presents data sets collected during wave guided experiments carried out at the Air Force Institute of Technology in Warsaw. The paper includes a description of test objects used during the measurements. Signal processing methods and damage indicators used are also described. Finally, the architecture of the database, which was developed to facilitate the work with the data sets, is illustrated.

1 Introduction

The article includes a description of the benchmark collection that will allow the reader to use it to conduct their research. The datasets were prepared for 9 objects, differing in the conditions of the measurements, the type of introduced fault, the material type, and the structure geometry. The structure of this article is as follows: section 2 describes the experiments carried out, section 3 presents a description of the calculated indices, and section 4 is devoted to the description of the database architecture.

2 Experiments

Nine experiments were performed as part of the research:

- 3 long-term temperature tests with simultaneous introduction of artificial defects,
- 3 laboratory fatigue tests,
- 3 temperature tests with simultaneous introduction of Barely Visible Impact Damage (BVID) on composite specimens.

The following subsections contain detailed description.

2.1 Long-term temperature tests

2.1.1 Tests with the introduction of artificial defects No 1

A dural sample was prepared as object 1, which is a fragment of the PZL-130 Orlik wing covering. The specimen of dimensions 380 x 175 mm contains the following riveted parts: sheet metal, reinforcing cover for the edges of the inspection opening, and a fragment of the stringer in the section of its overlap joint. A network of 8 PZT sensors was installed on the surface of the specimen. Sensors T1, T2, T6, and T7 were placed on the two jointed sections of the stringer. Sensors T4 and T5 are installed on the overlay connecting the stringers. T3 and T8 sensors are located on the

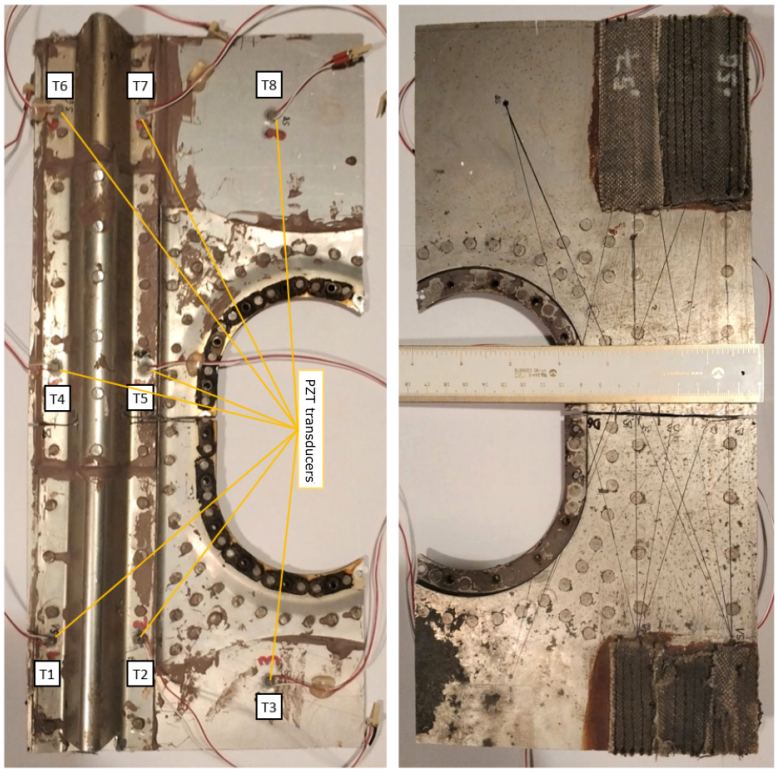

Figure 1: Test specimen with artificial defects (post-test condition).

sheathing. The test specimen with the installed network of PZT piezoelectric transducers in the state after the tests is presented in Fig. 1, where the marks of the damage introduction length for the given measurement series are also visible.

The thermal tests were carried out using a laboratory furnace. The sample with the leads was heated to the set temperatures and remained there also during the measurements. At the same time, the surface temperature of the test piece was measured using a thermocouple attached to the sample. Additional defects in the component were also introduced between selected measurement series. For this purpose, the sample was removed from the furnace and notched using a multi-sander and a cutting disc. The following excitation parameters for the piezoelectric transducers were used during the test:

- frequency of the excitation signal: 150 kHz,
- sampling frequency: 2.5 Mhz,
- signal length: 3 periods,
- type of signal modulation: Hanning window.

The table 1 summarises information on the damage parameters introduced before a given measurement series, the temperature ranges obtained during measurements of the PZT network. The description includes incremental damage measures and reference lengths relative to the nearest measurement paths.

Table 1: Conditions for a series of measurements during tests with the introduction of artificial defects No 1

Series No.	Description	Temp. min. [oC]	Temp. max. [oC]	Number of measuring cycles in the series
1	Reference measuring series. Undamaged sample.	29.6	67.5	18
2	Repetition of series 1.	27.8	67.6	18
3	Sheath cut to a length of 15 mm - D1. Cut tracks T1-T4 and T1-T6 - end of damage 1 mm behind the tracks	24.8	67	20
4	Enlarge the cut by 17 mm - D2. End of the damage at the intersection of paths T1-T7 and T3-T4, 8 mm after T2-T4, 10 mm before T2-T6.	29.3	67	12
5	Enlargement of the incision by 17 mm - D3. End of lesion 7 mm behind path T2-T6, 3 mm before T1-T5 path.	29.1	66.9	11
6	Enlargement of the notch by 10 mm - D4. Damage end 7 mm after T1-T5 path, 2 mm in front of intersection of paths T1-T8, T2-T5 and T2-T7. Cut in the stringer to thickness in the area under D4.	28.9	66.8	11
7	Enlargement of the incision by 12 mm - D5. End of defect at path T3-T5, 2 mm before crossing paths T1-T8, T2-T5 and T2-T7.	28.6	67.6	18
8	Repetition of series 7.	26.4	66.5	30
9	Enlargement of the incision by 15 mm - D6. Damage through the entire length of the plating.	28.4	66.5	15
10	Cut in the stringer at the flat side for a length of 7 mm - D7. End of damage (consistent with D1) on paths T1-T4 and T1-T6.	27.1	66	15
11	Widening of the stringer cut by 20 mm - D8. End of damage as per D2, at the intersection of paths T1-T7 and T3-T4.	28.6	67.8	25
12	7 mm long stringer cut on the reinforcement side (symmetrical to D7) - D9. End of damage at the intersection of paths T1-T8, T2-T5 and T2-T7. Measurement series shortened due to internal error of the measurement controller.	25.8	54.7	6
13	Repeated measurements for fault conditions as in series 12.	24.8	67	11
14	Increase of the notch of stringer D9 by 15 mm - D10. End of damage on path T1-T5.	25.5	65.7	11

2.1.2 Tests with the introduction of artificial defects No 2

In the second experiment for artificial defects and temperature changes, the specimen was a dural sample of the PZL-130 Orlik aircraft skin. The sample of dimensions 275 x 130 mm contains riveted along with fragments of plating, stringer and a frame placed perpendicularly to it. A network of 8 PZT sensors was installed on the surface of the specimen. Sensors T1, T3, T6 and T8 were installed on the plating. Sensors T2, T4, T5 and T7, on the other hand, are located on the plating. In addition, sensors T4 and T8 were located in the vicinity of the frame, on the opposite side of the frame than the other sensors. The specimen with the installed network of PZT piezoelectric transducers in the state after the tests is presented in Fig. 2, where the length markings of the introduced defect for the given measurement series are also visible.

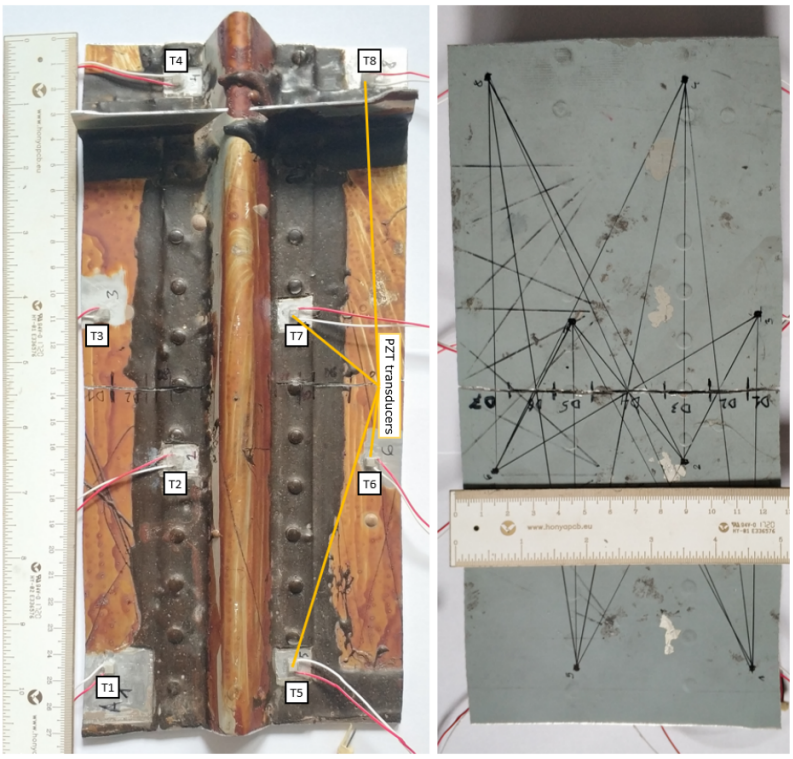

Figure 2: Sample No. 2 for testing with introduction of artificial defects (as tested).

Thermal tests were carried out both in a laboratory oven and when the sample was exposed to external conditions. The temperature was measured using a thermocouple attached to the surface of the specimen. In the case of tests in an outdoor environment, the readings of the temperature measuring apparatus were also verified using meteorological data. The following piezoelectric transducer excitation parameters were used during the test:

- frequency of the excitation signal: 150 kHz,
- sampling frequency: 2.5 MHz,
- signal length: 3 periods,
- type of signal modulation: Hanning window.

The table 2 summarises information on the damage parameters introduced before a given measurement series, the temperature ranges obtained during measurements of the PZT network. The description includes incremental damage measures and reference lengths relative to the nearest measurement paths.

Table 2: Conditions for a series of measurements during tests with the introduction of artificial defects No 2

Series No.	Description	Temp. min. [oC]	Temp. max. [oC]	Number of measuring cycles in the series
1	Measurement series in the laboratory oven. Sample undamaged.	25.4	66.4	19
2	Measurement series under outdoor conditions. Sample undamaged.	8.9	26.8	163
3	Series of measurements in laboratory oven. Undamaged specimen.	21.3	62.3	19
4	Repetition of series 3.	26.9	65.6	19
5	Repetition of series 3.	25.4	64	19
6	Measurement series in the laboratory oven. Sheath cut 12mm long - D1. End of damage 3mm behind path T1-T3.	24.3	64.2	30
7	Measurement series in laboratory furnace. Notch enlarged by 15mm - D2. End of the defect 4 mm behind the intersection of paths T1-T4, T2-T5 and T3-T5,	24.9	64.4	19
8	Measurement series in the laboratory oven. Enlargement of the notch by 19 mm - D3. Damage end 8 mm after T2-T4 path and 6 mm before path T2-T8.	24.1	63.8	19
9	Measurement series in the laboratory oven. Notch enlarged by 28 mm - D4. Longitudinal unbroken. End of plating damage 14 mm after intersection of paths T1-T8, T2-T7, T3-T6 and T4-T5. and 6 mm behind path T1-T7.	24.5	64.1	19
10	Measurement series in the laboratory oven. Increase of the notch by 15 mm - D5. End of defect 7 mm behind path T5-T7	25.5	66.7	23
11	Measurement series in the laboratory furnace. Notch enlarged by 17 mm - D6. Damage end 12 mm behind the path intersection T4-T6, T5-T8, T6-T7 and 5 mm before the T6-T8 path.	26.2	66.9	19
12	Measurement series in the laboratory oven. Enlargement of the notch by 19 mm - D7. Damage through the entire length of the plating. Longitudinal section undamaged.	26.4	66.4	21
13	Measurement series in outdoor conditions. No change in damage.	20	35.5	44
14	Series of measurements in a laboratory furnace. No defect changes.	24.5	66.2	23
15	Repeated series 14.	25.8	65.8	19
16	Series of measurements in the laboratory furnace. Notch in the stringer 5mm long, to the rivet - D8. Rivet scratched on the surface. Damage end 2-3 mm before the T2-T4 path through the centre of the rivet.	23.3	63.2	20
17	Measurement series in laboratory furnace. 12 mm enlargement of the stringer notch - D9. Damage end (congruent with D3) at the edge of the flat part of the stringer, 8 mm behind the T2-T4 path	24.8	64.2	19
18	Measurement series in the laboratory furnace. Notch in the other side of the stringer, 5 mm long, to the rivet - D10. Rivet undamaged. Damage end 2-3 mm before the T5-T7 path through the centre of the rivet.	25.4	63.4	19
19	Measurement series in laboratory furnace. Notch enlarged by 8 mm - D11. Damage end at the edge of the flat part of the stringer, 5 mm behind the T5-T7 path	25.2	63.4	19

2.1.3 Tests with the introduction of artificial defects No 3

The test specimen was a dural sample of the PZL-130 Orlik aircraft, analogous to the element used in test No. 2. The sample of 275 x 120 mm contains fragments of the plating, the stringer, and a frame placed perpendicularly to it, riveted together. A network of 8 PZT sensors was installed on the surface of the specimen. Sensors T1, T3, T6, and T8 were installed on the plating. Sensors T2, T4, T5, and T7 are also installed on the plating. In addition, sensors T1 and T5 were deployed adjacent to the frame, on the opposite side to the other sensors. The specimen with the installed network of PZT piezoelectric transducers in the state, after the tests are presented in Fig. 3, where the markings of the damage introduction length for the given measurement series are also visible.

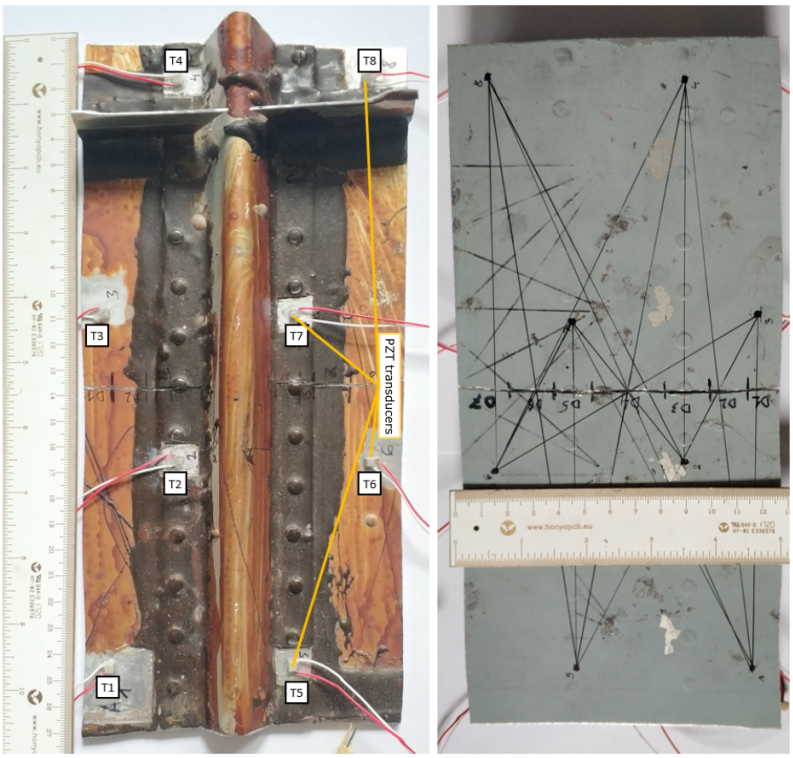

Figure 3: Sample No. 3 for testing with introduction of artificial defects (as tested).

Thermal tests were carried out both in a laboratory oven and when the sample was exposed to external conditions. The temperature was measured using a thermocouple attached to the surface of the specimen. In the case of tests in an outdoor environment, the readings of the temperature measuring apparatus were also verified using meteorological data. The following piezoelectric transducer excitation parameters were used during the test:

- frequency of the excitation signal: 150 kHz,
- sampling frequency: 2.5 MHz,
- signal length: 3 periods,
- type of signal modulation: Hanning window.

The tables 3 and 4 summarises information on the damage parameters introduced before a given measurement series, the temperature ranges obtained during measurements of the PZT network. The description includes incremental damage measures and reference lengths relative to the nearest measurement paths.

Table 3: Conditions for a series of measurements during tests with the introduction of artificial defects No 3

Series No.	Description	Temp. min. [oC]	Temp. max. [oC]	Number of measuring cycles in the series
1	Measurement series under outdoor conditions. Sample undamaged.	10.9	23.3	64
3	Series of measurements under outdoor conditions. Intact sample.	12	21.6	60
4	Series of measurements under outdoor conditions. Undamaged specimen.	9.2	19	60
5	Short term repetition of series 3.	14.6	15	2
6	Measurement series under outdoor conditions. Sample undamaged.	10.6	19.3	180
7	Measurement series under outdoor conditions. Sample undamaged.	6.2	9.8	180
8	Measurement series under outdoor conditions. Undamaged specimen.	9.8	10.9	5
9	Series of measurements under outdoor conditions. Undamaged specimen.	5.6	10.4	180
10	Series of measurements in the laboratory oven. Undamaged specimen.	22.4	62.4	45
11	Series of measurements in the laboratory furnace. Undamaged specimen.	23.5	62.4	45
12	Series of measurements in the laboratory oven. Undamaged specimen.	26.3	63.1	45
13	Series of measurements in the laboratory oven. Notch in plating 9mm long - D1. End of damage on path T1-T3.	29.1	60.7	40
14	Repetition of run 13.	26	63.1	40
15	Measurement series in the laboratory furnace. Enlargement of the notch by 19 mm - D2. End of defect 7 mm behind path T3-T5, 5 mm behind path T2-T3 and 3 mm behind path T1-T4.	37.6	62.3	40
16	Measurement series in the laboratory oven. Increase of the notch by 19 mm - D3. Damage end 8 mm behind path T2-T4 and 8 mm in front of path T2-T8.	25	62.7	40
17	Measurement series in the laboratory furnace. Notch enlarged by 27 mm - D4. Longitudinal unbroken. End of plating damage 14 mm after intersection of tracks T2-T7, T3-T6, T4-T5, 10 mm after track T1-T8 and 6 mm after track T1-T7.	24.9	62	40
18	Measurement series in the laboratory oven. Increase of the incision by 15 mm - D5. End of defect 6 mm behind path T5-T7	24.1	62.9	40
19	Measurement series in the laboratory furnace. Notch enlarged by 18 mm - D6. Damage end 12 mm behind the path T4-T6 and 9 mm after the intersection of paths T5-T8 and T6-T7, 3 mm in front of T6-T8 path.	24.9	62.7	40
20	Measurement series in the laboratory oven. Increase of the incision by 12 mm - D7. Damage through the entire length of the plating. Longitudinal section undamaged.	24	62.8	40
21	Series of measurements under outdoor conditions. No change in damage.	4.3	11.6	114
22	Series of measurements under outdoor conditions. No change of defect.	8.4	11.4	150
23	Series of measurements under outdoor conditions. No change in defect.	7.2	8.4	60
24	Series of measurements under outdoor conditions. No change in defect.	8.4	9.3	60
25	Series of measurements in a laboratory furnace. No defect changes.	18.9	58.5	42
26	Series of measurements in the laboratory furnace. Notch in the stringer 7 mm long - D8. End of damage on path T2-T4.	20.3	59.6	42
27	Measurement series in the laboratory furnace. Notch enlarged by 8 mm - D9. End of the defect (congruent with D3) at the edge of the flat part of the stringer, 8 mm behind the T2-T4 path	20.4	60	42
28	Measurement series in the laboratory furnace. Incision of the other side of the stringer 7 mm long - D10. End of the damage on path T5-T7.	22.1	59.5	42

Table 4: Conditions for a series of measurements during tests with the introduction of artificial defects No 3

Series No.	Description	Temp. min. [oC]	Temp. max. [oC]	Number of measuring cycles in the series
29	Measurement series in the laboratory furnace. Notch enlarged by 8 mm - D11. Damage end (consistent with D4) at the edge of the flat part of the stringer, 8 mm behind path T5-T7	20.3	58.9	42
30	Measurement series under outdoor conditions. No damage changes.	-0.5	15.5	123

2.2 Laboratory fatigue tests

2.2.1 Fatigue tests No 1

A dural sample was prepared for the test (Fig. 4), which is a fragment of the PZL-130 Orlik aircraft wing covering. The sample of dimensions 205 x 290 mm consists of a sheet of plating with two stringers riveted to it, oriented parallel to the shorter edges of the sample. To ensure fatigue damage propagation in the desired cross-section of the specimen, notches were introduced into the plating in the form of a 10 mm longitudinal notch. A network of 8 PZT transducers was installed on the specimen. The sensors were placed four at a time, symmetrically on both stringers between the rivets attaching them to the plating.

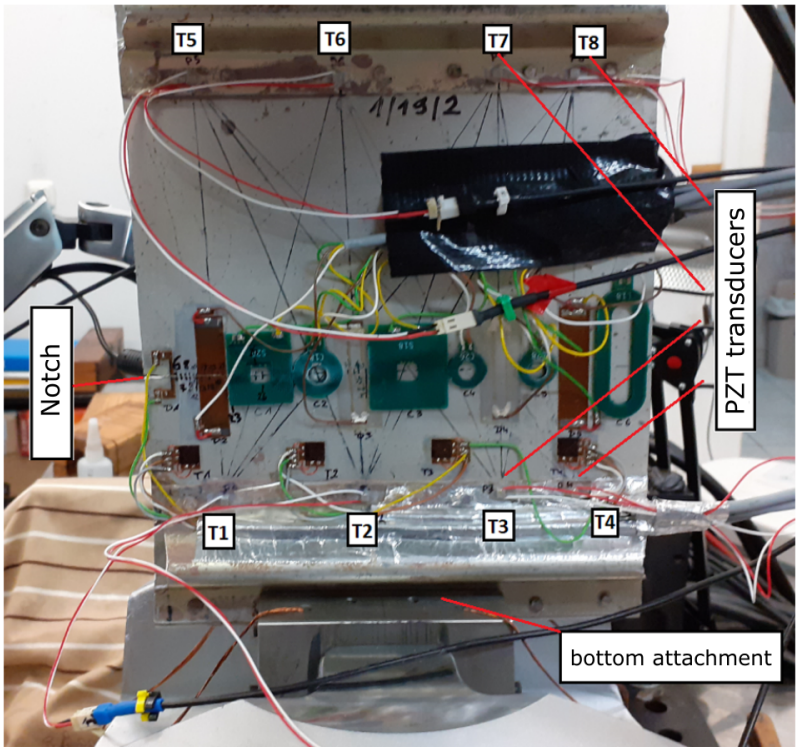

Figure 4: Fatigue test specimen 1 in the testing machine.

During the test, crack growth was inducted by cyclically stretching the specimen by applying a sinusoidal load with an asymmetry factor of 0.1, with the maximum force dependent on the current size and rate of crack growth. During the test, as the damage progressed, it was necessary to move the location of the specimen in the grips of the testing machine to ensure controlled propagation conditions. The specimen was moved in time between the specified measurement series so that the end of the damage did not exceed the mid-point of the gripping width. During the test, the current crack size was verified both visually and using a defectoscope. The end of the crack was continuously marked on the flat side of the specimen for reference to the test track system.

Measurement series for PZT networks were performed at selected crack lengths, after stopping the fatigue cycles. Within a single series, measurements were carried out in two states, for which constant loading forces were set equal respectively to 0 N and the maximum load obtained in the preceding fatigue cycles. PZT network measurements were carried out for each pair of transducers (measurement path) installed on the specimen. The following excitation parameters of the piezoelectric transducers were used during the test:

- frequency of the excitation signal: 150, 250 kHz,
- sampling frequency: 2.5 MHz,
- signal length: 3 periods,

- the type of signal modulation: Hanning window,

The tables 5 and 6 summarises the length of the introduced defects for each measurement series performed. The description takes into account both incremental measures and reference lengths in relation to the nearest measurement paths. Moreover, the indications of the ambient temperature sensor during the execution of measurements of a given series were also determined. The values of maximum forces obtained in preceding fatigue cycles and translated into static load at which the piezoelectric network was tested were also recorded.

Table 5: Conditions for measuring series during fatigue test 1.

Series No.	Description	Temp.[oC]	Maximum load [N]
1	Preliminary serie.	23.1	8
2	Reference serie after final positioning of sample in machine holder	22.9	8
3	Repetition of serie 2.	23	8
4	After initial fatigue cycles. No damage development.	22.7	8
5	After further fatigue cycles. No damage development.	23.2	8
6	Crack approximately 6 mm long from the notch end.	22.8	8
7	2 mm crack growth.	23.1	8
8	2 mm crack increment.	23.2	8
9	Increase in crack by approx. 1 mm.	23.2	8
10	Increase in crack by approx. 1 mm.	23.3	8
11	After specimen repositioning in the fixture. No change in failure.	25.8	8
12	Increase crack by approx. 1 mm.	23.8	8
13	2 mm crack increment.	23.4	8
14	Repeat the serie 13 No change in failure.	23.3	8
15	Repeat of serie 13.	23	8
16	Repeat measurement 13 at higher ambient temperature. No change in defect.	25.7	8
17	Crack growth 2 mm.	24	8
18	2 mm crack increment. 3 mm in front of path T1-T5.	23.7	8
19	Crack increment of 1.5 mm. 1 mm before T1-T5 path.	23.4	8
20	Crack increment of 3 mm. 2 mm behind track T1-T5.	23.1	8
21	After further fatigue cycles. No evident crack growth.	23.1	8
22	Repeat of serie 21. No damage development.	23.7	8
23	4 mm crack growth.	24.1	8
24	Crack increment of 8-9 mm. 3 mm in front of path T1-T6.	24.7	8
25	Crack increment of 2-3 mm, up to path T1-T6	24.5	8
26	Crack increment of 3 mm. 3 mm behind path T1-T6.	23.7	8
27	Crack increment of 3 mm.	25.6	8
28	2 mm crack increment.	25.2	8
29	2 mm crack increment	25	8
30	9 mm crack increment approx. 2 mm before path T1-T7.	23.2	8
31	Crack increment of 3 mm, up to path T2-T5. 1 mm behind path T1-T7.	24.7	8
32	Crack increment of 3-4 mm.	25.7	7
33	Crack increment of 3 mm. approx. 2 mm before path T1-T8.	23.6	7
34	After moving the specimen in the fixture. No change in damage.	25.1	8
35	Repeated measurement 34.	22.4	8
36	4 mm increment of crack. 1-2 mm behind path T1-T8.	23.6	8
37	Crack increment of 3 mm. approx. 4 mm before T2-T6 path.	25.6	8
38	Crack increment of 3-4 mm. 1 mm before the T2-T6 path.	25.9	8
39	Crack increment of 3-4 mm. 2 mm behind the T2-T6 path.	25	8
40	Crack increment of 2-3 mm.	24.7	7
41	Crack increment of 3 mm.	25	7
42	Crack increment of 10-11 mm. 1 mm before T3-T5 path, 3-4 mm before T2-T7 path	25.3	7
43	Repeated serie 43 No change in damage.	23.6	7
44	Sheath crack increase of 3 mm. 2 mm beyond path T3-T5, 1 mm beyond path T2-T7	24.3	6
45	Crack increment of 5 mm. 4 mm before T2-T8 path	25.2	6
46	Crack increment of 4 mm, up to path T2-T8.	25.3	6
47	Crack increment of 3 mm. 3 mm beyond T2-T8 path	23.8	6
48	Crack increment of 4 mm. 1 mm before path T3-T6.	25.8	5.5
49	Crack increment of approx. 2.5 mm. 2 mm after T3-T6 path, 2 mm before T4-T5 path	24.7	5.5
50	Crack increment of 2-3 mm, up to T4-T5 path.	26.2	5
51	Crack increment of 4 mm. 5 mm beyond T4-T5 path.	24.3	5
52	Crack increment of approx. 6 mm.	23.7	5

Table 6: Conditions for measuring series during fatigue test 1.

Series No.	Description	Temp.[oC]	Maximum load [N]
53	After moving the specimen in the fixture. No change in damage.	24.3	8
54	Crack growth of approx. 2.5 mm. 4 mm in front of path T3-T7.	24.4	8
55	Crack increment of approx. 4.5 mm. 1 mm after T3-T7 path, 1 mm before T4-T6 path	25.6	8
56	Crack increment of 3 mm. 2 mm after T4-T6 path, 5 mm before T3-T8 path	25.9	7
57	Crack increment of 3-4 mm. 2 mm before T3-T8 path.	25.9	7
58	Crack increment of 2-3 mm. 1-2 mm behind the T3-T8 path.	25.7	6.5
59	Crack increment of 3 mm.	26.3	6
60	Crack increment of 3 mm. Possibility of incorrect readings from first measurement.	25.7	6
61	Repeated serie 60 No change in failure.	22.6	6
62	4-5 mm crack growth. 2 mm in front of path T4-T7.	23.6	5.5
63	2 Crack increment of 3 mm. 1 mm behind the T4-T7 path.	23.9	5
64	Crack increment of 3 mm. 6 mm before path T4-T8.	23.9	5
65	Crack increment of 2-3 mm. 3 mm before the T4-T8 path.	24.4	4.5
66	Crack increment of 3 mm, up to T4-T8 path.	25.0	4.5
67	Crack increment of 3-4 mm.	24.5	4
68	Crack increment of 4 mm.	25.1	3.5
69	10 mm crack increment.	23.7	3

2.2.2 Fatigue tests No 2

A dural sample was prepared for the test, which is a fragment of the PZL-130 Orlik aircraft wing covering. The specimen of dimensions 385 x 170 mm contains a sheet of plating riveted together, an overlay reinforcing the edges of the inspection opening, and a fragment of the stringer in the section of its overlap joint. A 10 mm longitudinal notch was introduced from the edge of the plating to provide a suitable location for fatigue damage development in the initial phase of the test. During the test it was also necessary to add additional artificial flaws on the reinforcement and stringer, which was also done by notching. A network of 8 PZT sensors was installed on the specimen. Sensors T1, T2 and T7 and T8 were deployed on the two jointed sections of the stringer. Sensors T4 and T5 are installed on the overlay connecting the stringers. Sensors T3 and T6, on the other hand, are located on the sheath. A photograph of the test specimen placed in the grip of the testing machine is shown in Fig. 5, where the locations of the PZT piezoelectric transducers and the initial notch of the sheathing are also marked.

During the test, damage growth was introduced by cyclically stretching the specimen by applying a sinusoidal load with an asymmetry factor of 0.1, with the maximum force depending on the current size and rate of damage growth. Crack propagation during the test was monitored visually, including using a microscopic camera. The end of the crack at the measurement points was continuously marked on the currently damaged specimen element in order to relate the defect length to the measurement path system. Measurement series for PZT networks were conducted at selected crack lengths, after fatigue cycles were stopped and a static tensile force of 500 N was applied. PZT network measurements were carried out for each pair of transducers (measurement path) installed on the specimen.

The following excitation parameters of the piezoelectric transducers were used during the test:

- frequency of the excitation signal: 150 kHz,
- sampling frequency: 2.5 MHz,
- signal length: 3 periods,
- the type of signal modulation: Hanning window,

During the test to ensure controlled test conditions, as the damage progressed, it was necessary to change the location of the specimen in the grips of the testing machine.

The tables 7 and 8 summarises the length of the introduced defects during the tests for a given measurement series. Both incremental measures and reference lengths with the nearest measurement paths have been considered. Furthermore, the indications of the ambient temperature sensor during the measurements of a given series have also been determined. All measurements were carried out with a static load of 500 N.

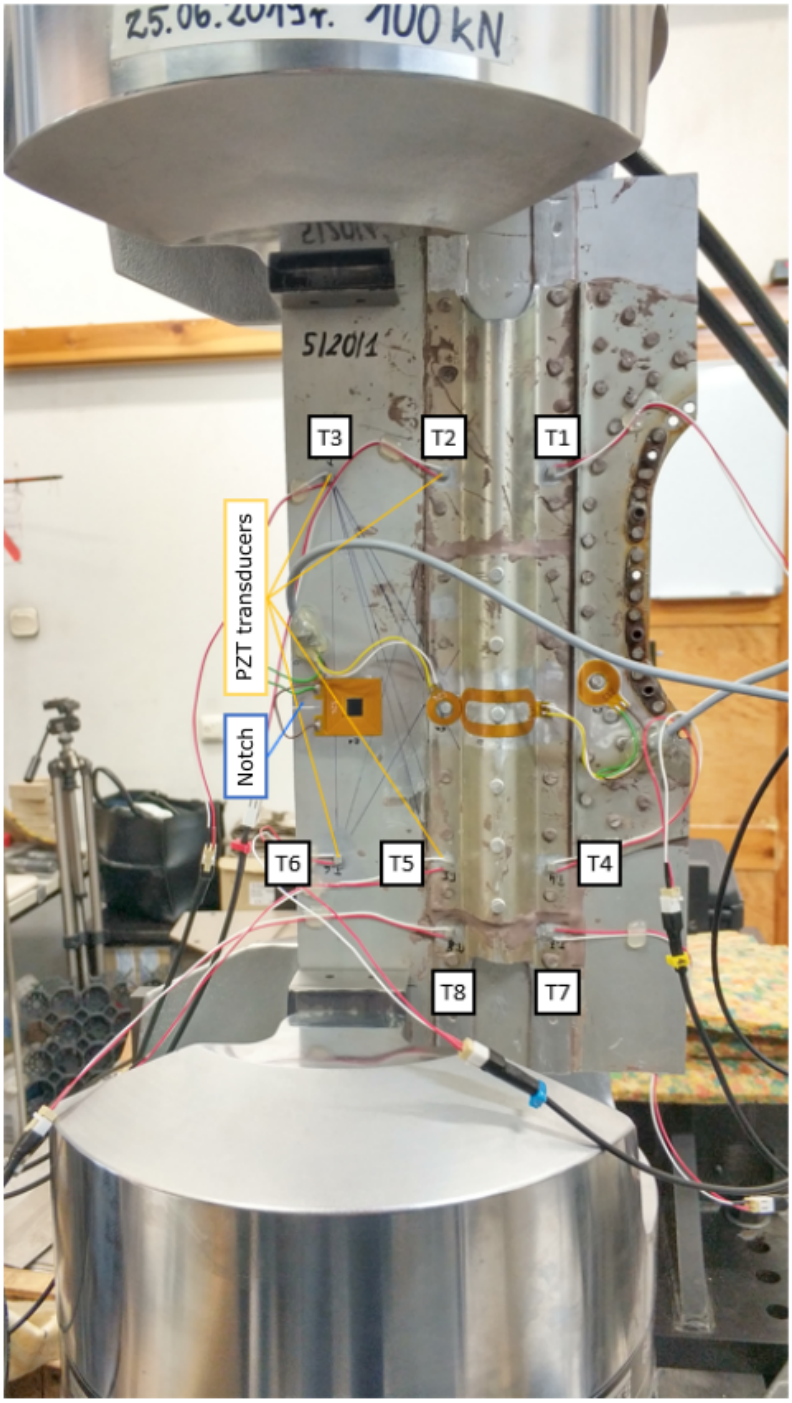

Figure 5: Fatigue test specimen 2 in the testing machine.

Table 7: Conditions for measuring series during fatigue test 2.

Series No.	Description	Temp.[oC]
1	Reference serie. Sample clamped behind plating	25
2	Repetition of serie 1.	25
3	Repeated serie 1.	22
4	Sheathing crack 5 mm from notch. 4 mm in front of path T3-T6.	25
5	Sheath crack growth of 4 mm, up to path T3-T6.	26
6	Repeated serie 5.	27
7	Repeated serie 5.	22
8	Crack increment of 3 mm beyond path T3-T6.	23
9	Crack increment of 4 mm.	24
10	9 mm increment of crack. 4 mm before path T2-T6.	26
11	4 mm sheath crack increment to path T2-T6. 4 mm in front of path T3-T8.	26
12	Crack increment of 4 mm, to path T3-T8. 5 mm in front of path T3-T5.	25
13	Crack increment of 2-3 mm. 2-3 mm before T3-T5 path.	26
14	Crack increment of 2-3 mm, up to path T3-T5.	26
15	After displacement of plating in fixation. No change in damage.	23
16	Crack growth of 3 mm beyond path T3-T5.	24
17	4 mm crack increment. 3 mm in front of path T1-T6.	25
18	Crack increment of 3 mm to path T1-T6.	25
19	Crack increment of 4 mm beyond path T3-T5. 3 mm in front of the hole edge and 5 mm in front of paths T2-T5, T2-T8 and T3-T7.	25
20	Crack increment to hole edge. 4 mm behind paths T2-T5, T2-T8 and T3-T7.	26
21	After changing specimen fixation to shank at centre of stringer. No change in damage.	26
22	Displacement of specimen in the fixture by 25 mm after further fatigue cycles and no incremental damage. Interface - aluminium flat bar added to the fixation.	21
23	Damage propagation from a 4mm long hole, to a T3-T4 path.	23
24	4 mm crack growth beyond path T3-T4.	24
25	Repeated serie 24.	21
26	Crack increment of 3 mm.	22
27	After changing specimen fixture to grip at centre of stringer. No change in failure.	23
28	Crack increment of 24 mm behind path T3-T4. 4 mm in front of the hole edge and 7 mm in front of paths T1-T4 and T1-T7.	24
29	Crack increment into the hole. 3 mm behind paths T1-T4 and T1-T7.	24
30	Shift of the specimen in the grip by 25 mm. Grip for stringer and plating. Interface - aluminium flat bar added to the fixture. No change in damage.	25
31	Crack growth of 5 mm.	26
32	4-5 mm crack growth.	26
33	Crack increment of approx. 9 mm, up to the edge of the hole.	26
34	After changing specimen clamping to plating grip. No change in damage.	23
35	Crack growth to complete break of plating. No visible damage to stringer or reinforcing overlay.	24
36	Complete failure of reinforcing overlay. No visible damage to the stringer.	25
37	After changing specimen attachment to grip on stringer and plating (through interface). Induction of a notch on the stringer by scratching the surface with a scalpel.	25
38	Propagation of the stringer crack for approx. 4 mm into the opening on paths T1-T4 and T1-T7.	24
39	Propagation of a crack about 3 mm from the edge of the hole to the stringer bend.	25
40	Crack growth of approx. 6 mm measured along the surface of the material. Crack on the bended part of the stringer, 18 mm to the edge of the opening at the top.	25
41	4 mm crack growth.	26
42	4 mm crack increment.	26
43	After changing specimen mount to grip in centre of stringer. No change in failure.	27
44	Repeated measurement 43.	23
45	Crack growth of 3 mm.	24
46	Damage propagation on the other side of the stringer 2-3 mm from the hole towards the edge of the stringer - intersection of tracks T2-T5, T2-T8 and T3-T7 No changes to the original damage in relation to series No. 45.	26
47	After changing the grip of the specimen to the previous grip of the stringer and plating (through the interface). No change in damage.	27

Table 8: Conditions for measuring series during fatigue test 2.

Series No.	Description	Temp.[oC]
48	Increase in original damage by 3-4 mm. 3 mm to the edge of the opening at the top of the stringer. No change in damage at the opening on the other side of the stringer.	27
49	Increase of primary crack to opening at top of stringer. Secondary crack growth to edge of stringer - T1-T6 path intersection.	27
50	Propagation of crack from bottom hole to 5-6 mm from edge. Approx. 23 mm to the hole at the top. T3-T4 path intersection, end of damage 2-3 mm behind the path. No damage from top hole.	27
51	Repeated serie 50.	24
52	Increase of the crack by approx. 5 mm towards the top. No damage from the upper hole.	24
53	4 mm crack growth. No damage from the upper hole.	25
54	4 mm crack growth. No damage from the upper hole.	25
55	3-4 mm crack growth. 5-6 mm of undamaged material to edge of opening at top of stringer.	26
56	Measurements after breaking of the specimen and separation of fragments	25

2.2.3 Fatigue tests No 3

A steel specimen (Fig. 6), constituting a fragment of the wing spar of Su-22 aircraft, was prepared for testing. The specimen, measuring 370 x 122 mm, was made from a single block of HSA40 stainless steel, containing a fragment of the spar flange along with a wall section adjoining it, cut off at a height of approximately 60 mm. To mechanically weaken the specimen, the girder wall was cut at the location of the desired fatigue failure. A section of the flange was also cut to equal its thickness to the thinnest section found at the riveted joints. In addition, notches in the form of 1-2 mm long were also introduced at the edge of the specimen and the edges of the hole near it. A network of 8 PZT types was installed on the specimen (Fig. 6). Sensors T1, T3, T5, and T7

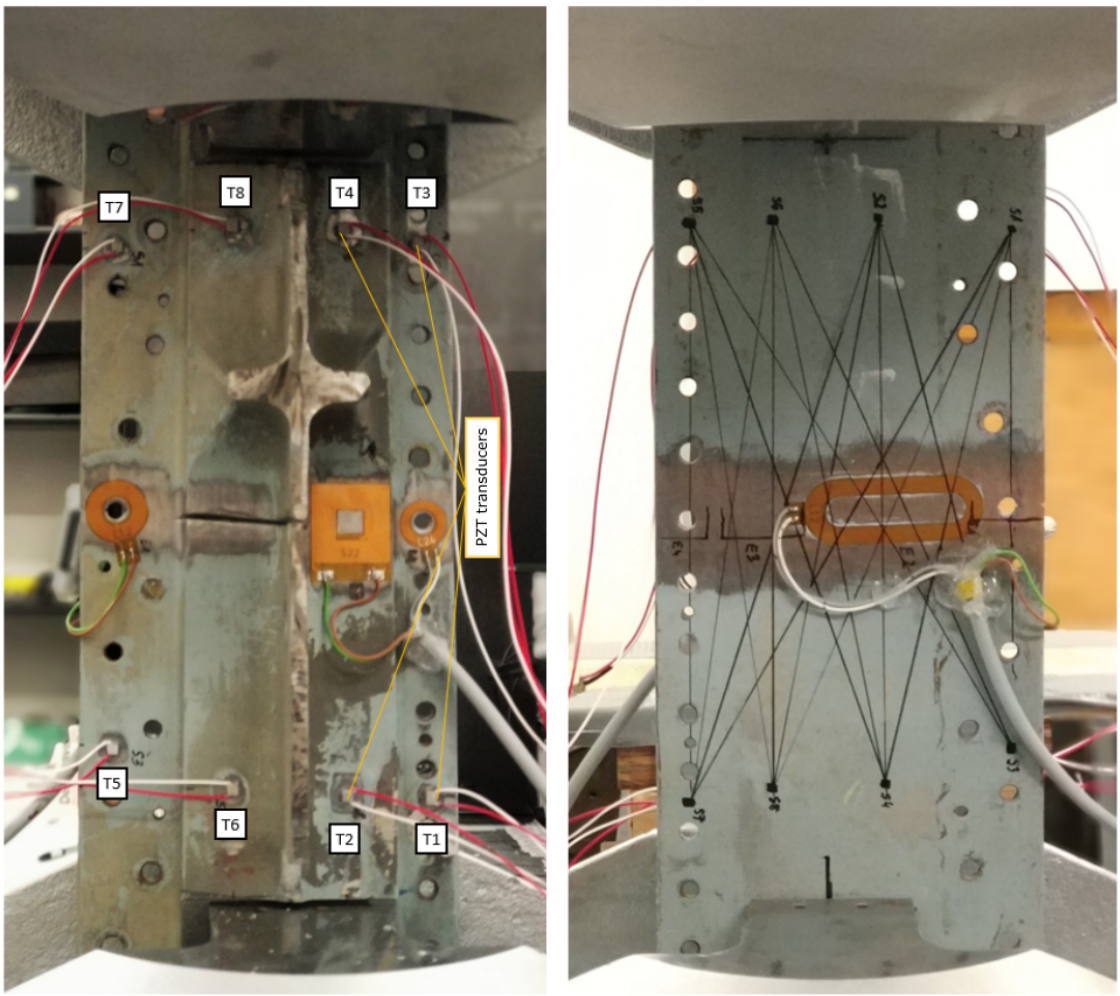

Figure 6: Fatigue test specimen 3 in the testing machine.

were deployed on sections of lesser thickness, on the rivet line. Sensors T2, T4, T6, and T8 were installed on the main part of the girder flange. The additional transverse notch was introduced on the path between sensors T6 and T8 to weaken the specimen. During the test, crack growth was inducted by cyclically stretching the specimen by applying a sinusoidal load with an asymmetry factor of 0.1, with the maximum force dependent on the current size and rate of crack growth. During the test, as the damage progressed, it was necessary to move the specimen's location in the grips of the testing machine to ensure controlled propagation conditions. The specimen was moved within the width of the main flange of the girder, i.e. within +/- 10 mm relative to the centreline of the member. Crack propagation during the test was monitored visually, using a microscopic camera. The end of the crack at the measurement points was continuously marked on the surface of the flat side of the specimen to relate the defect length to the measurement

path system. Measurement series for PZT network were conducted at selected crack lengths after the fatigue cycles had stopped. Measurements of the PZT network were performed for each pair of transducers (measurement path) installed on the specimen. For each accepted crack length two series of measurements were carried out in two static load conditions: 0 N and 10 kN or the maximum load obtained in previous fatigue cycles (if less than 10 kN). At the last seven test points, the tests were carried out exclusively without applying any force due to the potential possibility of premature specimen rupture under constant load. The following excitation parameters of the piezoelectric transducers were used during the test:

- frequency of the excitation signal: 150 kHz,
- sampling frequency: 2.5 MHz,
- signal length: 3 periods,
- the type of signal modulation: Hanning window,

Tables 9 and 10 summarises the results of the analysis of the location of the end of the introduced damage for a given measurement series of the PZT network. Both incremental measures on both sides of the sample and reference lengths relative to the nearest measurement paths have been taken into account. Furthermore, the ambient temperature value during the measurements of a given series were also determined. The values of forces at which the tests of a given measurement series were performed are also listed.

Table 9: Conditions for measuring series during fatigue test 3.

Series No.	Description	Temp.[oC]	Maximum load [N]
1	Reference measurement.	25.6	0
2	Repetition of serie 1.	25.5	0
3	After the initial fatigue cycles. No damage development.	25.9	0
4	Repeated serie 3. 24.8 0		
5	Repeated serie 4 under load.	25.1	10
6	After further fatigue cycles. No damage development.	26.2	0
7	Repeated serie 6 under load.	26.2	10
8	After further fatigue cycling. No damage development.	26.3	0
9	Repeated serie 8 under load.	26.2	10
10	Repeated serie 8.	23.6	0
11	Repeated serie 10 with load.	24.3	10
12	After notch enlargement and specimen displacement in the holder.	25.0	0
13	Repeated the serie 12 under load.	24.8	10
14	Crack into the opening at half the specimen thickness side of the notch - flat side of the specimen.	26.0	0
15	Repeated serie 14 under load.	25.7	10
16	Crack to hole on T1-T3 path (approx. 9 mm specimen width) through entire thickness.	26.0	0
17	Repeated serie 16 under load.	26.2	10
18	24.08 Repeated series 16.	24.6	0
19	Repeat serie 18 under load.	24.4	10
20	Increase in crack by approx. 4 mm from hole.	24.9	0
21	Repeat serie 20 under load.	25.1	10
22	Occurrence of a surface crack in a notch at the height of the girder wall. Increase of crack from rivet by 5 mm. End 3 mm before T2-T3 path.	24.9	0
23	Repeat serie 22 under load.	26.6	10
24	Repetition of serie 20 after opening and closing again the lower grip of the machine. The transition of the crack in the notch to the other side of the specimen was detected (possibly already present in 22): section from 1 mm behind path T1-T4 to 1 mm behind path T3-T6 (cut). Total length of the second damage: 12 mm. post 25.9 -. con.	26.5	0
25	Repeat serie 24 under load.	25.8	10
26	Increase of crack from rivet side by 2 mm - 1 mm before path T2-T3. Increase of crack from notch: - on one side 2 mm, end 1 mm before T2-T3 path, T1-T4 path cut; - on the other side 4 mm, end on path T1-T8 2 mm of material left to join the cracks.	25.6	0
27	Repeat serie 26 under load.	25.4	10
28	Repetition of serie 25.	25.0	0
29	Fracture joint - interrupted T2-T3 path No change in position of crack ends on the flat side of the specimen. On the inner side, damage propagation up to 1 mm behind the notch end, 3 mm behind the wall side. Total crack length 68 mm	25.6	0
30	Repeated serie 29 under load.	25.6	10
31	Increase crack on flat side by 3-4 mm, to path T2-T4 No change on the inner side.	25.6	0
32	Repeated serie 31 under load.	25.6	10
33	Increase of crack on flat side by 4 mm, 1 mm after breaking of path T3-T5. No change on the inner side.	25.7	0
34	Repeated serie 33 under load.	25.1	10
35	Repeated serie 33.	25.5	0
36	Repeated serie 35 with load.	26.1	10
37	On flat side, crack growth of 4 mm to path T1-T7. No change on the inner side.	27.0	0
38	Repeated serie 37 under load.	25.7	10
39	On the flat side a 4 mm crack increment. End of damage 4 mm before cutting of paths T2-T8 and T4-T6. No lesion on the inner side.	27.0	0
40	Repeated serie 39 under load.	27.4	10
41	On the flat side, 4 mm crack increment; 1 mm after the T2-T8 path and 1 mm before the T4-T6 path. No change on the inner side.	25.2	0
42	Repeated serie 41 under load.	25.1	10
43	On flat side 2 mm increment of crack; 1 mm behind path T4-T6. No change on inner side.	25.5	0
44	Repeated serie 43 under load.	25.2	10
45	After moving the specimen in the holder. No change in damage.	23.2	0
46	Repeated serie 45 with load.	23.8	10
47	Repetition of serie 45	23.7	0

Table 10: Conditions for measuring series during fatigue test 3.

Series No.	Description	Temp.[oC]	Maximum load [N]
48	On flat side 6 mm crack increment; 3 mm in front of T4-T5 path. No change on the inner side.	24.4	0
49	Repeated serie 48 under load.	24.1	10
50	On flat side 3-4 mm crack increment; T4-T5 path broken; 2 mm before T6-T8 path. T6-T8. On inner side propagation of damage under current sensor E3; Increment of 4-7 mm.	24.3	0
51	Repeated serie 50 at load.	24.2	10
52	On flat side 5 mm crack increment; 2 mm behind the T6-T8 path. On the inner side, propagation by 12 mm relative to point 29; not possible to accurately relate to the condition of point 29. 50	24.4	0
53	Repeat of serie 52 under load.	24.2	10
54	Repeat of serie 52.	23.1	0
55	Repeated serie 54 with load.	23.5	10
56	Crack increment of 6 mm on flat side; 3 mm behind T5-T8 path. On the inner side an increment of approx. 4 mm.	24.2	0
57	Repeated serie 56 under load.	24.1	10
58	After moving the specimen in the holder. No change in damage.	24.2	0
59	Repeated serie 58 under load.	24.4	10
60	On flat side 4 mm crack increment; at intersection of T5-T8 and T6-T7 tracks. On the inner side an increment of about 5-6 mm under sensor E5.	24.3	0
61	Repeated serie 60 under load.	24.5	10
62	Repeated serie 60.	22.3	0
63	Repeated serie 62 with load.	22.3	10
64	4 mm crack growth on flat side. On the inner side an increment of approx. 8 mm; Descent of the crack to a thin section. 17 mm to end of specimen	25.8	0
65	Repeated serie 64 under load.	25.4	7
66	After further fatigue cycles. No incremental damage.	24.5	0
67	Repetition of serie 66.	24.4	0
68	Repetition of serie 68 under load.	24.8	7
69	On flat side 4 mm crack increment; 2 mm to edge of hole. On the inner side an increment of 2-3 mm under the sensor E4.	26.1	0
70	Repeated serie 69 under load.	26.3	7
71	Damage propagation on both sides of specimen to the hole on path T5-T7.	24.9	0
72	After insertion of notch in hole wall to a depth of 1 mm and further fatigue cycles. No visible damage propagation.	24.5	0
73	Repeated serie 72.	23.6	0
74	2 mm crack propagation on flat side; 5 mm to end of specimen On the inner side an increment of 1-2 mm under the sensor E4.	23.9	0
75	Repetition of serie 74.	21.8	0
76	Repeated serie 74.	24.3	0
77	On flat side crack propagation of 3 mm; 2 mm to end of specimen On the inner side an increase of up to 3 mm before the end of the specimen	25.8	0

2.3 Temperature tests with BVID

In this study, a glass-fiber reinforced composite panel was used, equipped with PZT piezoelectric transducers embedded in the network structure, from which signals were collected at varying temperatures, either by heating the samples with halogen lamps or during exposure to atmospheric conditions, so that the temperature stability of PZT network readings could be investigated. The signals were collected for a specific number of measurement cycles. One measurement cycle included data acquisition for all pairs of network transducers. The remaining measurement series were performed for one repetition of the measurement cycle. Three-panel areas (Fig. 7) containing PZT transducer networks of eight sensors, were selected for the series of experiments. The geometry of the PZT network was analogous for each area tested.

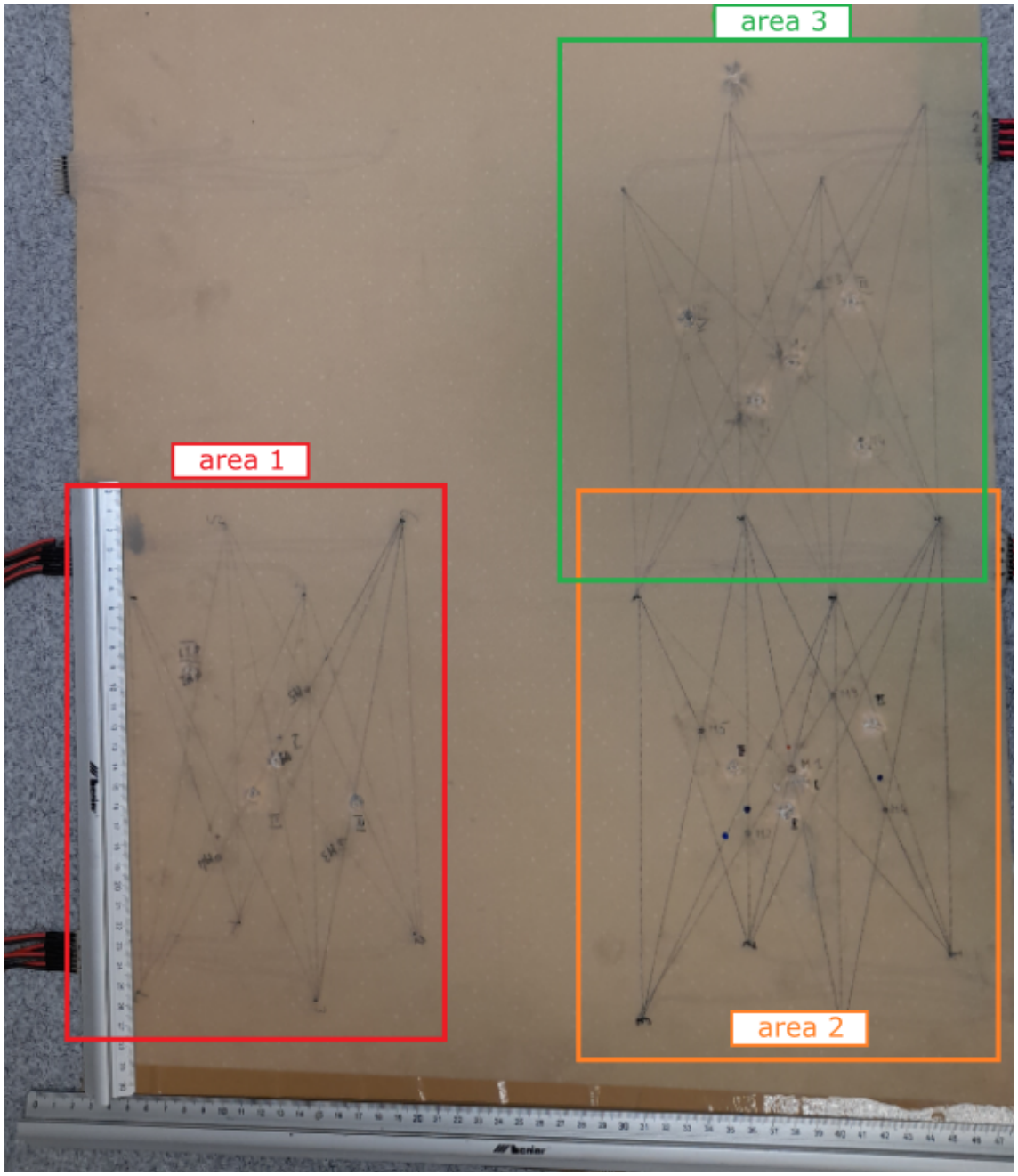

Figure 7: Composite panel with embedded networks of PZT transducers with marked test areas.

BVID-type impact damage was introduced between selected measurement series using an air

Table 11: Conditions for a series of measurements in a BVID experiment for sample No. 1

Series No.	Description	Temp. min. [oC]	Temp. max. [oC]
1	Measurement series under outdoor conditions. Undamaged sample.	-4	1
2	Series of measurements under outdoor conditions. Sample undamaged.	-2	3
3	Measurement for an undamaged sample at room temperature.	25	26
4	Repeat of measurement series no. 3.	25	26
5	Measurement for sample with inserted mass element at location No. 1	25	26
6	Measurement for sample with inserted mass component at location No. 2	25	26
7	Measurement for sample with inserted mass element at location No. 3	25	26
8	Measurement for the sample with mass component in location 4	25	26
9	Measurement for the sample with inserted mass component at location No. 5	25	26
10	Measurement for an intact sample at room temperature.	25	26
11	Repetition of measurement series No. 10.	25	26
12	Measurement after introducing the first BVID defect	25	26
13	Measurement after introducing the second BVID defect	25	26
14	Measurement after entering the third BVID fault	25	26
15	Measurement at elevated temperature	40	41
16	Measurement at room temperature	23	24
17	Measuring series in outdoor conditions after entering the fourth BVID fault	0	-1
18	Measuring series at outdoor conditions	-1	0
19	Measurement at room temperature	22	23
20	Measurement at elevated temperature	37	39
21	Measurement at elevated temperature	64	68

rifle. The impact energy was below 17J. The temperature of the specimen during testing was measured using a pyrometer. Before introducing the impact damage, measurements were also performed for the introduced artificial defect, simulated by attaching a mass element to the specimens at selected locations within the network of the PZT transducers.

The following excitation parameters of the piezoelectric transducers were used during the test:

- frequency of the excitation signal: 150, 250 kHz,
- sampling frequency: 2.5 MHz,
- signal length: 3 periods,
- the type of signal modulation: Hanning window,

The photographs (Fig. 8a - Fig. 8c) show the location of impact damage within the PZT transducer network for the three tested samples, while the tables 11 - 13 present the conditions for performing the elastic wave measurement series.

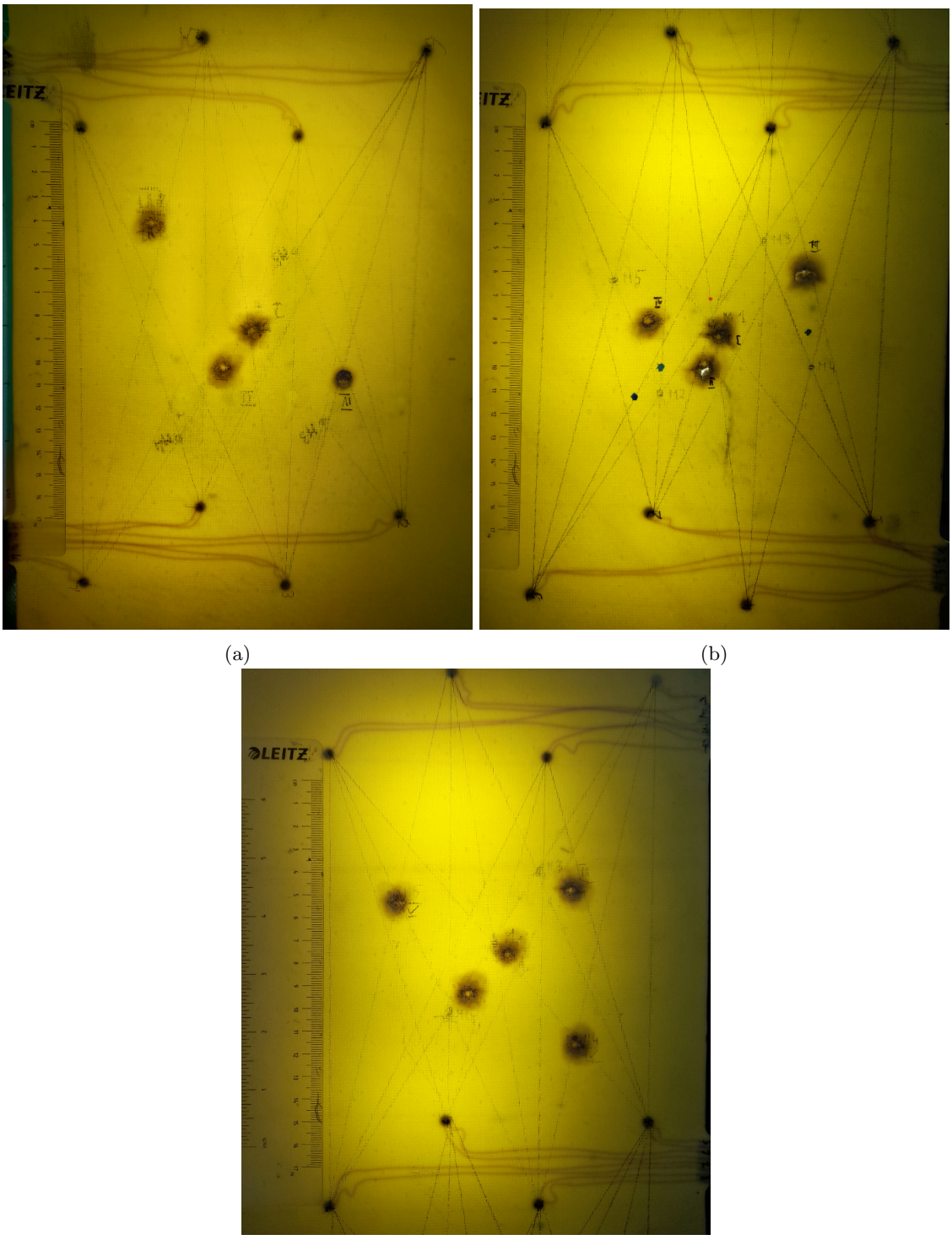

Figure 8: a) BVID damage image of sample No 1; b) BVID damage image of sample No 2; c) BVID damage image of sample No 3.

Table 12: Conditions for a series of measurements in a BVID experiment for sample No. 2

Series No.	Description	Temp. min. [oC]	Temp. max. [oC]
1	Measurement series under outdoor conditions. Undamaged sample.	-4	2
2	Measurement for an undamaged sample at room temperature.	21	22
3	Measurement at elevated temperature	41	43
4	Measurement at elevated temperature	66	70
5	Measurement for sample with mass component inserted at location No. 1	21	22
6	Measurement for sample with mass component inserted at location No. 2	21	22
7	Measurement for sample with mass component inserted at location No. 3	21	22
8	Measurement for the sample with mass component inserted at location 4	21	22
9	Measurement for the sample with mass component inserted at location No. 5	21	22
10	Measurement for an intact sample at room temperature	21	22
11	Measurement after first BVID damage	21	22
12	Measurement at elevated temperature	41	43
13	Measurement at elevated temperature	68	72
14	Measurement series under outdoor conditions.	1	2
15	Measurement series in outdoor conditions after entering the second BVID defect	0	1
16	Measurement at room temperature	21	22
17	Measuring at elevated temperature	42	44
18	Measuring at elevated temperature	67	71
19	Measuring after entering the third BVID fault	21	22
20	Measurement at elevated temperature	66	70
21	Measurement at elevated temperature	46	50
22	Measurement series in outdoor conditions.	3	4
23	Measurement series in outdoor conditions after introducing the fourth BVID defect	2	3
24	Measurement at room temperature.	22	23

Table 13: Conditions for a series of measurements in a BVID experiment for sample No. 3

Series No.	Description	Temp. min. [oC]	Temp. max. [oC]
1	Measurement series under outdoor conditions. Undamaged sample.	-2 2	
2	Series of measurements under outdoor conditions.	0 1	
3	Repeat measurement series No. 2	0	1
4	Measurement in room of moderate temperature	13	14
5	Measurement at room temperature	19	20
6	Measurement at elevated temperature	47	51
7	Measurement at elevated temperature	34	38
8	Measurement at room temperature	19	20
9	Measurement for sample with mass component at location No 1	19	20
10	Measurement for sample with mass component in location 2	19	20
11	Measurement for sample with inserted mass component at location 3	19	20
12	Measurement for a sample with a bulk element inserted at location 4	19	20
13	Measurement for a sample with mass component inserted at location No. 5	19	20
14	Measurement at room temperature after introduction of first BVID damage	19	20
15	Measurement at room temperature	13	14
16	Measurement at elevated temperature	34	38
17	Measurement at elevated temperature	52	56
18	Measurement series in outdoor conditions.	-1	2
19	Measurement at elevated temperature	29	33
20	Measurement at room temperature	19	20
21	Repeat of measuring series No. 20	19	20
22	Measurement at room temperature after introduction of the second BVID defect	18	19
23	Repeat of measurement series No. 22	18	19
24	Measurement in a room at a moderate temperature	14	15
25	Measurement series in outdoor conditions.	3	4
26	Measurement at elevated temperature	44	48
27	Measurement at elevated temperature	32	36
28	Measurement at elevated temperature	56	60
29	Measurement at room temperature	18	19
30	Repeat of measurement series No. 29	18	19
31	Measurement at room temperature after introduction of the third BVID failure	18	19
32	Repeat of measurement series No 31	18	19
33	Measurement at room temperature after introduction of the fourth BVID failure	18	19
34	Repeat of measurement series No. 33	19	20
35	Measurement at room temperature after introduction of the fifth BVID failure	19	20
36	Repeat of measurement series No 35	19	20

3 Signal processing algorithms and labels

The collected sets of raw signals were processed to calculate damage-sensitive indices. For this purpose, each signal was subjected to the following procedure. The first step was preprocessing which included detrending and bandpass filtration. After this step, each signal was matched with a baseline signal. To perform this task, two diffent approaches were applied: simple baseline selection and optimal baseline selection. From these processed signals, damage indices were calculated. Finally, the calculated indicator values were subjected to a post-processing procedure to mini.

3.1 Preprocessing

The pre-processing of the signals consisted of two steps. The first was to remove the fixed trend which was related with mean value subtraction.

Next, the signal was filtered to reduce the frequency components in the spectrum. For this purpose, a band-pass window filter with zero phase shift was used. The filter bandwidth was limited by two frequencies 1000 Hz and 400000 Hz.

3.2 Baseline selection

The analysis of the recorded waveforms is a difficult task. For a given excitation frequency of the PZT transducer, numerous modifications of these waves with different propagation velocities may coexist simultaneously, which makes the analysis of the recorded signals difficult. Moreover, for structures with complex geometry, containing numerous sources of elastic wave scattering, e.g. riveted joints. The degree of complication of the obtained signals increases significantly, which makes it impossible to diagnose the structure solely on the basis of the current signal. Therefore, a comparative analysis of signals recorded for the current state of the structure with baseline signals obtained for the initial state is used.

To select the reference signal, two different approaches were used: simple baseline selection and optimal baseline selection [1]. Both use the pre-processed signals and information about the PZT sensor pairs for which they were acquired.

Simple baseline selection Based on a small number of reference signals. The first signal assigned to a given PZT transducer pair is selected.

Optimal baseline selection Based on a set of reference signals. Firstly an algorithm selects signals set that is assigned to a given pair of PZT transducers. From this set, the most simmilar signal is selected. The selection criterion is the average distance between the inspected signal and the reference one.

3.3 Damage indicators

For purpose of guided waves folowing features were calculated from signals [2, 3]:

- DI_{CO} - Pearson Cross-correlation estimate ($\widehat{R}_{xy}(0)$) obtained between the baseline (x) and the signal (y) for the lag equal to 0,

$$DI_{CO} = 1 - \frac{\widehat{R}_{xy}(0)}{\sqrt{\widehat{R}_{xy}(0)\widehat{R}_{yy}(0)}} \tag{1}$$

- DI_{HEN} - Normalized squared error between envelopes of the signal and the baseline. Envelopes (X(t) and Y(t)) are calculated using Hilbert transform,

$$DI_{HEN} = \frac{\int_{t_1}^{t_2} |Y(t) - X(t)|^2 dt}{\int_{t_1}^{t_2} X(t)^2 dt} \tag{2}$$

- DI_{IP} - damage index which compensate the temperature influence based on instantaneous phase of signal calulated using Hilbert transform. The phase of the signal $y(t)$ can be modified

simply using the following relation

$$y'(t) = y(t)e^{i(\phi_x - \phi_y)} \tag{3}$$

where ϕ_x is instantaneous phase of the baseline $x(t)$. Damage index is defined as.

$$DI_{IP} = 1 - \frac{\widehat{R}_{xy'}(0)}{\sqrt{\widehat{R}_{xy'}(0)\widehat{R}_{y'y'}(0)}} \tag{4}$$

- DI_{RMS} - Normalized squared error between the signal ($y(t)$) and the baseline ($x(t)$).

$$DI_{RMS} = \frac{\int_{t_1}^{t_2} |y(t) - x(t)|^2 dt}{\int_{t_1}^{t_2} x(t)^2 dt} \tag{5}$$

- DI_{XCO} - Maximum value of Pearson cross-correlation estimate obtained for all possible lags (τ)

$$DI_{XCO} = 1 - max(\frac{\widehat{R}_{xy}(0)}{\sqrt{\widehat{R}_{xy}(0)\widehat{R}_{yy}(0)}}) \tag{6}$$

3.4 Post-processing

Post-processing was carried out to minimise the spurious values of the indices, related to the measurement errors. It is assumed that for a given pair of tranducers, e.g. PZTA and PZTB, the approximate equality can be satisfied [4].

$$DI_{Xn}(PZTA, PZTB) = DI_{Xn}(PZTB, PZTA) \tag{7}$$

where $DI_{Xn}(PZTA, PZTB)$ are index values for signal $n-th$ that PZTA was the generator and PZTB the receiver, and at $DI_{Xn}(PZTB, PZTA)$ PZTB was the generator and PZTA the receiver. Concidering the relation 7, the value of the index estimated as

$$DI_{Xn} = min(DI_{Xn}(PZTA, PZTB), DI_{Xn}(PZTB, PZTA)). \tag{8}$$

To exploit the relation 7, the indicators were grouped into sets. For the sets formulation, two criteria were applied regarding the signal for which the indicator values were calculated. The first one was related to the identifier of the measurement series. The second one was the identifiers of the PZT transducers.

The grouped indicators were used to calculate the minimum values. For this purpose, a pair of indicators $DI_{Xn}(PZTA, PZTB)$ and $DI_{Xn}(PZTB, PZTA)$ were selected from the grouped set of values. The indicator value was calculated from the following relation 7. In order to further reduce measurement errors, the calculated minima were grouped into 6 pairs. The the algorithm calculated the minimum value of the indicators as

$$DI_{Xn,\ldots,n+5} = min(DI_{Xn}, DI_{Xn+1}, DI_{Xn+2}, DI_{Xn+3}, DI_{Xn+4}, DI_{Xn+5}) \tag{9}$$

3.5 Signal labels

Based on the the experiments description presented in section 2, the labels of the signals contained in the sets were determined. The labels are assigned on the basis of pairs of PZT transducers, whose mutual position determines the shortest path for guided waves and the distance of such path from the damage. Regarding these informations, the assigned labels take the following values:

- 3 - for the path away from the damage, whose normalised distance satisfies the inequality:

$$d_{norm} = \frac{d_{dmg,(PZTA,PZTB)}}{d_{(PZTA,PZTB)}} > 0.25 \tag{10}$$

- 2 - for the path away from the damage whose normalised distance from the damage meets the inequality:

$$d_{norm} = \frac{d_{dmg,(PZTA,PZTB)}}{d_{(PZTA,PZTB)}} \leq 0.25 \tag{11}$$

- 1 - for the path passing through the damage.

where $d_{dmg,(PZTA,PZTB)}$ is the shortest distance between the defect and the path and $d_{(PZTA,PZTB)}$ is the distance between the transducers.

4 Database architecture

The database SYPIN_database.db was developed to facilitate the work with the described sets of signals presented in section 2. It consists of 14 tables, which contain information that allows convenient processing of measurement signals, development of labels, and storage of calculated index values. The database consists of the following tables.

- Table **db_paths** information about relative paths to signals acquired during measurement as well as experiment description files is stored. To work with the dataset, the file structure in the database folder should be similar to that shown in Fig. 9a. The processing_methods and signal_features_labels folders contain information about processing algorithms and fault indicators, which are described in section 3. The SYPIN_experiments folder contains the unprocessed signals, arranged in 9 subfolders shown in Fig. 9b.

(a) (b)

Figure 9: a) Folders structure; b) Subfolders structure.

- In table **experiments** experiment description is stored. The table for the experiment contains 9 record. The records placed correspond to the following experiments:
  - SYPIN_lab_experiment_1, SYPIN_lab_experiment_2 and SYPIN_lab_experiment_3 correspond in turn to the experiments described in section 2.1;
  - SYPIN_fatigue_experiment_1, SYPIN_fatigue_experiment_2 and SYPIN_fatigue_experiment_3 correspond successively to the experiments described in section 2.2;
  - SYPIN_BVID_experiment_1, SYPIN_BVID_experiment_2 and SYPIN_BVID_experiment_3 correspond successively to the experiments described in section 2.3.
- In table **monitored_objects** description of monitored objects in the experiment is stored. The table for the experiment contains 9 record.
- In table **sensors** information about sensor network is stored, their type, identfier and position in space [mm]. The sensor position information was used to generate signal labels.

- In table **measurement_conditions_labels** informations about conditions labels which were controlled during signal acquisition are stored. For the all experiments, the following measurement conditions were defined:
  - excitation frequency [kHz];
  - ambient temperature [^oC];
  - load [kN] -load exerted on the structure during measurements.
  - excitation gain – label indicates whether the signal applied to the transducer has been additionally amplified [0/1].
- In table **measurement_conditions** informations about external conditions for measurement are stored.
- In table **measurement_series_conditions_labels** informations about measurement conditions labels which were controlled during acquisition series are stored. For the all experiments, the following measurement series conditions were defined:
  - crack_no_n_pos_X_1 [mm], crack_no_n_pos_Y_1 [mm], crack_no_n_pos_X_2 [mm], crack_no_n_pos_Y_2 [mm] – the approximate position of the vertices of the n-th crack. This information was used to generate signal labels;
  - ambient temperature [^oC];
  - max. ambient temperature [^oC];
  - min. ambient temperature [^oC];
  - load [kN] -load exerted on the structure during measurements.
  - mass_no_1_pos_X_1 [mm], mass_no_1_pos_Y_1 [mm], mass_no_1_diameter [mm] – the approximate position of the centre and the diameter of the mass simulating the damage. This information was used to generate signal labels;
  - BVID_no_n_pos_X_1 [mm], BVID_no_n_pos_Y_1 [mm], BVID_no_n_diameter [mm] – the approximate position of the centre and the diameter of the n-th BVID. This information was used to generate signal labels.
- In table **measurement_series_conditions** informations about external conditions for measurement series are stored.
- In table **measurement_series** context informations about conducted series of measurements are stored. Detailed information on the measurement series can be found in section 2.
- In table **measurements** information about performed measurements during the experiment are stored. The sensor_id column contains a reference to the transmitter and the receiver_id column to the receiver.
- In table **signal_processing_methods** informations about methods for signal processing are stored. For the experiment table contains 3 records:
  - **raw_signals** which refers to acquired signals;
  - **detrend_simple-filter_bandpass-simple_baseline_selection-min_postproc** which refers to processing described in section 3;
  - **detrend_simple-filter_bandpass-optimal_baseline_selection-min_postproc** which refers to processing described in section 3;
- In table **processed_signals** references to signals acquired during the experiment and processed are stored.
- In table **signal_feature_labels** informations about types of calculated features are stored. For the experiment table contains 6 records:
  - **lw_co** - the damage index, which is calculated from the following equation 1

  - **lw_hen** - the damage index, which is calculated from the following equation 2
  - **lw_ip** - the damage index, which is calculated from the following equation 4
  - **lw_rms** - the damage index, which is calculated from the following equation 5
  - **lw_xco** - the damage index, which is calculated from the following equation 6
  - **damage_distance_3class** - signal labels described in section 3.5

- In table **signal_features** information about calculated features values and labels values are stored.
- In table **signal_features_parameters** information about calculated features parameters are stored. This table does not contain any records.

5 Summary and conclusions

The article provides information on the benchmark set. The objects and the course of experiments that were used to develop the set of signals are described. The topic related to signal processing was discussed. The signal processing algorithm, calculated damage indicators, and developed labels assigned to signals are described. Finally, the structure of the database is presented. Some of the tables with the records in them were described.

References

[1] Y. Lu and J. E. Michaels, "A methodology for structural health monitoring with diffuse ultrasonic waves in the presence of temperature variations," *Ultrasonics*, vol. 43, no. 9, pp. 717–731, 2005.

[2] L. Ambrozinski, P. Magda, K. Dragan, T. Stepinski, and T. Uhl, "Temperature compensation based on Hilbert transform and instantaneous phase for Lamb waves-based SHM systems of aircraft structures," *Structural Health Monitoring 2013: A Roadmap to Intelligent Structures - Proceedings of the 9th International Workshop on Structural Health Monitoring, IWSHM 2013*, vol. 1, pp. 1259–1266, 2013.

[3] Z. Dworakowski, K. Dragan, and T. Stepinski, "Artificial neural network ensembles for fatigue damage detection in aircraft," *Journal of Intelligent Material Systems and Structures*, vol. 28, no. 7, pp. 851–861, 2017.

[4] K. Dragan and M. Dziendzikowski, "A method to compensate non-damage-related influences on Damage Indices used for pitch-catch scheme of piezoelectric transducer based Structural Health Monitoring," *Structural Health Monitoring*, vol. 15, no. 4, pp. 423–437, 2016.